GPR Data Simulation for Detecting Subsurface Bodies

Dr. Hussein H. Karim
Building and Construction Engineering Department, University of Technology/ Baghdad
Email: husn_irq@yahoo.com
Haidar A. N. Al-dami
Engineering College, University of Al-Qadisiya/ Al-Diwaniya

Received on: 11/10/2011 & Accepted on: 5/4/2012

ABSTRACT

Ground-penetrating radar (GPR) technique was used at University of Technology-Baghdad, as a non destructive, quick, low cost and powerful technique in detecting any change in the constituents of subsurface as materials which can be consequently applied in urban and constructed areas. The main objectives of this study are: to simulate GPR data obtained by 250 and 500 MHz antennas for shallow engineering investigation by detecting different subsurface bodies. A simulation is made for GPR data with different geometric buried bodies and located at different depth. Before processing, most of the raw data of radargram do not reflect the presence of the buried bodies. But after processing by using suitable filters and other interpretation tool parameters, many of the investigated subsurface bodies and structures appeared clearly. It is found from this study that the degree of clarity of the buried bodies do not depend on the higher value of dielectric constant of the body, but it depends on the contrast between the body and the host medium. Thus the body with low dielectric constant appears more clear than that with higher dielectric constant, when they are at the same depth. Most of the buried bodies appeared on GPR radargrams using the medium frequencies. The best detecting depth are 1.5 m to 1 m for 250 and 500 MHz antennas respectively.

Keywords: Ground penetrating radar, Data simulation, Dielectric constant, Antenna frequency, Buried bodies

محاكاة بيانات الرادار الأرضي لاستكشاف الأجسام تحت السطحية

الخلاصة

استخدمت تقنية الرادار الأرضي في موقع الجامعة التكنولوجية في بغداد كتقنية لا اتلافية وسريعة وقليلة الكلفة وذات قدرة تمييز عالية لاستكشاف اي تغير في مكونات المواد تحت السطحية والتي يمكن استخدامها في المناطق المدنية والمشيدة. تهدف الدراسة الحالية الى محاكاة بيانات الرادار الأرضي المستحصلة بهوائيات ذات ترددات 250 و500 ميكاهيرتز للاستكشافات الهندسية الضحلة من خلال التحري عن الأجسام تحت السطحية المختلفة. تم عمل محاكاة لبيانات الرادار الأرضي مع أجسام هندسية مختلفة مدفونة باعماق مختلفة. وقبل المعالجة ، لم تظهر البيانات الأصلية للمخططات الرادارية وجود هذه الأجسام المدفونة. ولكن بعد المعالجة وباستخدام المرشحات المناسبة و معاملات التفسير، ظهر بوضوح العديد من الأجسام والتراكيب تحت السطحية المراد التحري عنها . وجد من هذه الدراسة بان درجة وضوح الأجسام المدفونة لا تعتمد

https://doi.org/10.30684/etj.30.15.9
2412-0758/University of Technology-Iraq, Baghdad, Iraq

على القيم الأعلى لثابت عزل الجسم ولكنها تعتمد على مقدار التغاير بين الجسم والوسط المضيف. وعليه فالجسم ذو ثابت العزل الواطئ يظهر بوضوح أكبر من الجسم ذو ثابت العزل العالي عندما يكونان بنفس العمق. ظهرت معظم الأجسام المدفونة في المخططات الرادارية باستخدام الترددات المتوسطة. وكان أفضل عمق استكشافي هو 1.5 و 1 متر للهوائيات ذات الترددات 250 و 500 ميكاهيرتز على التوالي.

INTRODUCTION

Ground-penetrating radar (GPR) also known as ground probing radar, impulse radar or subsurface interface radar, is a geophysical technique used for high resolution imaging the subsurface and it is a non-destructive technique can consequently be applied in urban and sensitive environments [1,2]. GPR is the general term applied to techniques which employ radio waves, typically in the 1 to 1000 MHz frequency range, to map structure and features buries in the ground or in man-made structures [3]. It is sensitive to changes in all three electromagnetic characteristics of a medium, electric permittivity, electric conductivity, and magnetic permeability [4].

GPR uses electromagnetic propagation and back scattering to image, locate, and quantitatively identify changes in electrical and magnetic properties in the ground. It has the highest resolution in subsurface imaging of any geophysical method, approaching centimeters. Detecting of subsurface feature depends upon contrast in the dielectric, electrical and magnetic properties. Interpretation of ground-penetrating radar data can lead to information about depth, orientation, size, and shape of buried objects, and soil water content [5].

GPR is often used in one of two ways depending on the aim of the survey. First as a real-time locator tool in which the antenna is moved around the area of interest, objects are detected directly on the real-time screen and marked as they are noted. Second as a mapping tool in which the antenna is moved over the site in a grid system and the data is, after the survey, loaded into a more advanced interpretation tool such as 3-D imaging software [6].

Ground-Penetrating Radar (GPR) transmits and records reflected electromagnetic energy. In the GPR method, a transmitter is used to send electromagnetic energy into the ground, then from geologic interfaces where a dielectric contrast exists. The reflected energy is recorded by a receiver and produces a picture of the reflected waves.

The aim of this study is to make a simulation between GPR data, obtained by 250 and 500 MHz antennas, with shallow engineering investigation by detecting different subsurface bodies.

THEORETICAL BACKGROUND

Operation and Modes of Data Acquisition

GPR measurements are based on the transmission and reflection of an electromagnetic wave in the studied medium [7]. The radar system causes the transmitter antenna (TX) to generate a wavetrain of radiowaves which propagates away in a broad beam [8]. Variation in the electrical properties of the subsurface cause part of the transmitted signal to be reflected and this reflected signal is

detected by the receiver [9]. Several waves may reach the receiver antenna [10], as shown in figure (1). The ground wave is that propagating directly from the transmitter to the receiver through the ground, the air wave is that which travels directly between the transmitter and receiver antennas, the reflected waves represent energy returned directly at a boundary while refracted waves occur when a change in electrical property is encountered and the wave travels along the interface and consequently arrives later than its corresponding reflected wave [11]. The permittivity of water is high compared to dry materials, so the water content and porosity are important controls on penetration [1].

Propagation of Radiowaves

Ground radar radiation is electromagnetic radiation and its propagation is described by Maxwell's equations [8]. Velocity and attenuation are the factors that describe the propagation of high-frequency radiowaves in the ground [9] .

Velocity

Electromagnetic waves travel at a specific velocity determined primarily by the permittivity of the material. The relationship between the velocity of the wave and material properties is the fundamental basis for using GPR to investigate the subsurface. The velocity is different between materials with different electrical properties, and a signal passed through two materials with different electrical properties over the same distance will arrive at different times [12]. The speed of radiowaves (V_m) in any medium is dependent upon the speed of light in free space (c=0.3m/ns), the relative dielectric constant (ϵ_r) and the relative magnetic permeability (μ_r= 1 for non-magnetic materials) and is given by [9]:

$$V_m = c \,/\, \sqrt{\left\{\left(\frac{\epsilon_r\, \mu_r}{2}\right)[(1 + P^2) + 1]\right\}} \qquad (1)$$

Radar signal velocity in low-loss geological materials ($P \approx 0$) which are amenable to radar sounding is related to ϵ_r by

$$V_m = c/\sqrt{\epsilon_r} \qquad (2)$$

The relative dielectric constant (ϵ_r) varies from 1 in air to 81 in water. For most geologic material, ϵ_r lies in the range 3 – 30. Consequently, the range of radiowave velocities is large from around 0.06 to 0.175 m/ns [8] (Fig. (2)).

Energy Loss and Attenuation

Energy loss of radiowaves occurs as a consequence of reflection / transmission losses about each interface, a further loss of energy is caused by the geometrical spreading of the energy. The radar signal is transmitted in a beam with a cone angle of 90º. As the radio signals travel away from transmitter, they spread out causing a reduction in energy per unit area at rate of $1/r^2$, where r is the distance traveled as shown in Figure(3).

The attenuation is the fundamental cause of energy loss. The attenuation factor (α) is dependent upon the electric (σ), magnetic (μ) and dielectric (ϵ) properties of the media through which the signal is propagating as well as the frequency of the signal itself [8]:

$$\alpha = \omega\left\{\left(\frac{\mu\epsilon}{2}\right)\left[\left(1 + \frac{\sigma^2}{\omega^2\epsilon^2}\right)^{1/2} - 1\right]\right\}^{1/2} \quad (3)$$

Where $\omega = 2\pi f$, f is the frequency (Hz), μ is the magnetic permeability ($4\pi \times 10^{-7}$ H/m), σ is the bulk conductivity at the given frequency (S/m), ϵ ($= \epsilon_r \epsilon_0$) is the permittivity and ϵ_0 is the permittivity of free space (8.854×10^{-12} F/m). The formula is valid for non-magnetic materials only. The term ($\sigma/\omega\,\epsilon$) above is equivalent to the loss factor (P), such that:

$$P = \sigma/\omega\epsilon \quad (4)$$

Also as with other electromagnetic waves, the depth by which the signal has decrease in amplitude to 37% of initial value is known as skin depth (δ) and is inversely proportional to the attenuation factor as [8].

$$\delta = 1/\alpha \quad (5)$$

GPR can be used providing the conditions are appropriate for the method. Clay in the soil will attenuate the GPR signal and severely limit depth penetration. The GPR signal is severely attenuated if the ground is electrically conductive. Ideal conditions are dry, sandy soils, although good results should be obtained in soils saturated with fresh (resistive) water. In ideal conditions, the method may penetrate to depths of 15 m.

Scattering

When a wave encounters a material with a different permittivity, then the electromagnetic energy will change direction and character. This transformation at a boundary is called scattering [12]. Scattering from thin layers or point-type objects like boulders decrease the radar signal amplitude and these losses are often included in the attenuation term [9].

The success of the GPR method relies on the ability of the ground to allow the transmission of radiowaves and the contrast in ϵ_r between adjacent layers that give rise to reflection of incident electromagnetic radiation this can be quantified using the amplitude reflection coefficient (R).

$$R = \frac{\sqrt{\epsilon_{r2}} - \sqrt{\epsilon_{r1}}}{\sqrt{\epsilon_{r2}} + \sqrt{\epsilon_{r1}}} \quad (6)$$

Where ϵ_{r1} and ϵ_{r2} are the relative dielectric constants in layers 1 and 2 respectively. This equation assumes no other signal losses [8].

When wave impinges on interface, it scatters the energy according to the shape and roughness of the interface and the contrast of electrical properties between the host material and the object. Part of the energy is scattered back into the host material, and the other portion of the energy may travel into, and through, the object.

STUDY AREA AND FIELD WORK

This study is carried out in the University of Technology site (Fig.(4)). To create simulation of field work for GPR survey, a hole has been excavated with dimension 3 m in length, 3 m in width and 1.25 m in depth (Fig.(5)) at the garden of Turning Unit. The soil at this site is wet and rich in roots of trees and other plants (Fig. 6). Different materials with different dimensions (Table (1)) and various electrical properties (dielectric constant and conductivity) are planned to be buried at three depth layers 1.25, 0.85 and 1.25 m as first, second and third layers respectively as shown in figure 7. Next, GPR with antennas 250 and 500 MHz is used along profiles perpendicular and longitudinal (parallel) to these buried bodies.

RESULTS AND INTERPRETATION

The processing and interpretation of buried bodies at different layer depths can be explained respectively from the bottom to the top layer as follows:

The first layer (at depth 1.25 m)

Using 500 MHz antenna

For the first layer, the raw data of radargrams do not reflect the presence of buried bodies (plastic pipe, ferrous pipe, wood prism, reinforced beam, concrete cubs and glass plate). But with the assistance of RadExplorer software these objects appear by processing with filters and using the spectrum and some interpretation tools such as hyperbola and line. To determine the dielectric constant and wave propagation velocity within the medium, the hyperbola and line tools were applied (RadExplorer 1.4, 2005). Radargrams for buried bodies using 500 MHz processed by RadExplorer software are shown in figure(8). Processing results of these bodies extracted from their radargrams are listed in Table(2).

Examining figure 8a, it is appeared that the degree of clarity is different among the various bodies. The plastic pipe is clearly appeared due to its size and the high dielectric contrast with the surrounding soil. It is characterized by its low dielectric constant and with high velocity of its reflected wave. This body faced interference with the cut edge anomaly of the hole test at its left side. Thus, the right side of its anomaly is present, so the line interpretation tool is used instead of the hyperbola tool to complete matching. The Ferrous pipe and reinforced beam are clearly appeared with respect to other objects also due to the high dielectric contrast with respect to the host soil surrounding it. Concerning the glass plate, it is well appeared due to its size (width) and high dielectric contrast. While, the woody prism except its right side does not appear due to the presence of huge roots of trees in the site so line interpretation tool is used instead of hyperbola tool. Concrete cubes are not clearly appeared.

Using 250 MHz antenna:

In the raw data of radargrams for the first layer, the buried bodies are appeared. But, these bodies cannot be interpreted using interpretation tools even after processing by filters due to their very simple appearance of these bodies as shown in figure (9).

The second layer (at depth 0.85 m)

Using 500 MHz antenna

For the second layer, the raw data of radargrams reflected the presence of buried bodies. After processing using spectrum tools, these bodies appeared with more clearance. To determine the dielectric constant and wave propagation velocity within the medium, the hyperbola and line were used for the radargrams of all buried bodies lying within this layer as shown in the figure (10). Information results extracted for these bodies are listed in table (3).

Examining figure 10a, as in the discussion of the first layer, it is obvious that the degree of clarity is different among various bodies. The plastic pipe is well defined due to its size and the high dielectric contrast with the host soil, as it is characterized by its low dielectric constant with high reflected wave velocity. Ferrous pipe and reinforced beam also clearly defined due to the high contrast with respect to the host soil. The glass plate is well appeared due to its size and high dielectric contrast. While, the woody prism is not well appeared due to huge roots of trees in the site as in the first layer. Concrete cubes are well defined in this case.

Using 250 MHz antenna

In the raw data of radargrams for the second layer, the buried bodies are not clearly defined, but after processing by filters they appeared as shown in figure(11).

The third layer (at depth 0.45 M)

Using 500 MHz antenna

For the third layer, the raw data of radargrams do not reflect the presence of the buried bodies. By applying the spectrum tool to the raw data of radargrams before processing, the bodies appeared clearly. To determine the dielectric constant and velocity within the medium, the hyperbola is used for all bodies within this layer as shown in the figure 12. The extracted information results of these bodies are listed in table 4.

As discussed for the first two layers, examining figure (12a) it is obvious that different clarity is obtained for various buried bodies. The plastic pipe is well defined due to its size and dielectric contrast. Ferrous pipe and reinforced beam are also clearly appeared for their high dielectric contrasts with respect to other bodies. The glass plate also is well defined for its size and dielectric constant. While, the woody prism is clearly appeared in the contrary to the other two layers. Concrete cubes are less appeared in comparison to second layer but with higher clarity compared to the first layer.

Using 250 MHz antenna

For the third layer raw data of radargrams, the buried bodies do not appear. But after processing by filter, these bodies well appeared and can be recognized without using RadExplorer software as shown in figure (13).

LONGITUDINAL GPR SURVEYING

The aforementioned surveys at hole site are perpendicular to the buried bodies. In this part, the GPR survey is longitudinal (parallel) to the buried objects. To do such survey, we made the surveying profiles much closer to each other about three times than that made for perpendicular surveying. However the buried bodies do not appear using the 250 and 500 MHz antenna. However, there is one object clearly appeared in the longitudinal surveying, which is the iron sewage pipe that was found in the hole site shown in figure 5 which extends along the hole about 80 cm from the edge and 80 cm depth. The appearance of this pipe is due to the direction of GPR surveying which is perpendicular to it as shown in the figure (14).

CONCLUSIONS

The main conclusion points can be summarized as follows:

1- GPR device is a suitable method that uses as non destructive low cost, quick technique survey, sensitive for the dielectric characters of the media through 2D radargrams of the subsurface applied in constructed area. These points make the technique powerful tool in detecting any change in the constituents of the subsurface materials.
2- Some obstacles related to ground condition can be overcome by utilizing some filters resulted in high resolutions after such processing.
3- Most of the raw data of radargrams before processing do not appear the presence of subsurface bodies and structures. But after processing and applying the suitable filter and other interpretation tool parameters, many of the investigated subsurface structures clearly appeared reflecting the high resolving power of the technique.
4- The degree of clarity of subsurface bodies does not depend on their higher dielectric constant, but on the dielectric contrast between the body and the host medium and the size of the body compared to the object buried bodies appeared in the same radargram.
5- The extracted information, after using processing with the assistance of RadExplorer software, shows that the dielectric constant and velocity of the buried bodies are approximately the same value as tabulated in published standard tables with difference ± 0.3 in dielectric constant
6- It is found that the best detecting depths for 250 and 500 MHz antennas are 1.5 and 1 m respectively at which the buried bodies appeared in the raw data without processing.

REFERENCES

[1] Kearey, P., Brooks, M. and Hill, I., "An Introduction to Geophysical Exploration", Third Edition, Blackwell Science Ltd., 2002.
[2] Griffin, S. and Pippett, T., "Ground Penetrating Radar. Geophysical and Remote Sensing Methods for Regolith Exploration", Vol.144, pp. 80-89, 2002.
[3] Anann A.P, " Ground Penetrating Radar Workshop Notes", Sensors & Software Inc., 2001.

[4] Sciotti M., Colone F., Pastina D. and Bucciarelli,T., "GPR for archaeological investigations real performance assessment for different surface and subsurface conditions", Proc. of IGARSS 03, pp. 2266-2268, 2003.
[5] US Army Crop of Engineers, "Engineering and Design Remote sensing, Engineering Manual", No. 1110-2-2907, 2003.
[6] Nissen,J., Johansson, B., Wolf Matthew J. W., Skoog, L., "Ground Penetrating Radar a ground investigation method applied to utility locating in no-dig technologies", Malå Geoscience Raycon Stockholm, pp. 1-6, 2001.
[7] Chanzy, A., Tarussov, A., Judge, A. and Bonn, F., "Soil water content determination using a digital ground-penetrating radar", Soil Science Society of America Journal, Vol. 60, pp. 1318-1326, 1996.
[8]Reynolds, J. M., "An Introduction to applied and environmental geophysics", West Sussex, John Wiley & Sons Ltd, 1997.
[9] Davis, J. L., and Annan, A.P., "Ground penetrating radar for high-resolution mapping of soil and rock Stratigraphy", Geophysical Prospecting, Vol. 37, pp. 531-551, 1989.
[10] Du S., and Rummel, P., "Reconnaissance studies of moisture in the subsurface with GPR", Proceedings of the Fifth International Conference on Ground Penetrating Radar, Kitchener, Ontario, 12-16 June 1994, 1241-1248, 1994.
[11] Charlton M.B., "Principles of ground-penetrating radar for soil moisture assessment", Journal of Hydrology review on 31st May 2006, 2006.
[12] Daniels, J., Ehsani, M. R., and Allred, B. I., "Handbook of agricultural geophysics", Chapter 7, Ground-Penetrating Radar Methods (GPR), pp.129-145, 2008.

Table (1) Specifications of buried materials.

No.	Material Type	Length	Width	Thickness
1	Plastic pipe	50 cm	15.24cm. (in diameter)	1 cm
2	Ferrous pipe	50cm	5.08 cm. (in diameter)	0.5 cm
3	Woody prism	50 cm	5.08 cm.	5.08 cm
4	Reinforced beam	50 cm	2.54 cm. (in diameter)	--------
5	Concrete cubes	45 cm	15 cm	15 cm
6	Glass plate	100 cm	16 cm	

Table (2) Materials information extracted by processing using Rad Explorer software at 1.25 m depth.

No.	Material Type	Depth (m)	(Eps)	standard	Velocity cm/ns
1	Plastic pipe	1.32	3	3	17.3
2	Ferrous pipe	1.34	14	14.2	8
3	Woody prism	1.34	4	4	15
4	Reinforced beam	1.31	14.3	14.2	8
5	Concrete cubes	1.27	7.9	8	10.6
6	Glass plate	1.38	4.9	5	13.4

Table (3) Material information extracted by processing using Rad Explorer software at 0.85 m depth.

No.	Material	Depth (m)	ϵ_r (Eps)	ϵ_r standard	Velocity (cm/ns)
1	Plastic pipe	0.86	3.2	3	17.3
2	Ferrous pipe	0.88	14.2	14.2	8
3	Woody prism	0.87	4	4	15
4	Reinforced beam	0.85	14.1	14.2	8
5	Concrete cubes	0.87	8	8	10.6
6	Glass plate	0.85	5.2	5	13.4

Table (4) Material information extracted by processing using RadExplorer software at 0.45 m depth.

No.	Material Type	Depth (m)	ϵ_r (Eps)	ϵ_r standard	Velocity cm/ns
1	Plastic pipe	0.41	3	3	17.3
2	Ferrous pipe	0.44	14	14.2	8
3	Woody prism	0.42	3.4	4	15
4	Reinforced beam	0.45	14	14.2	8
5	Concrete cubes	0.4	7.8	8	10.6
6	Glass plate	0.45	4.9	5	13.4

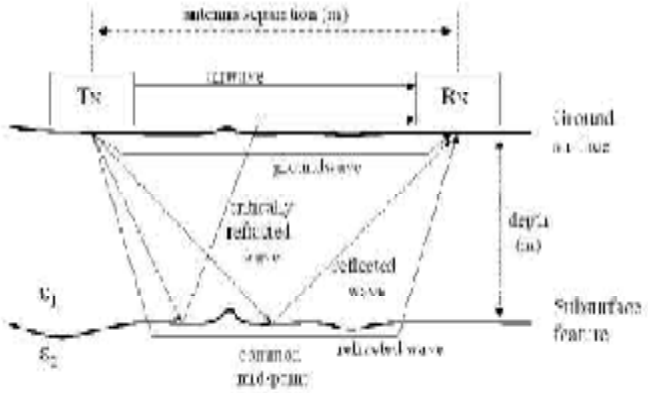

Figure (1). Waves reaching the receiver antenna [10].

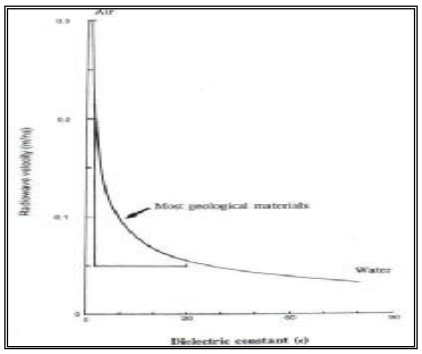

Figure (2) Dielectric constant as a function of Radio wave velocity [8].

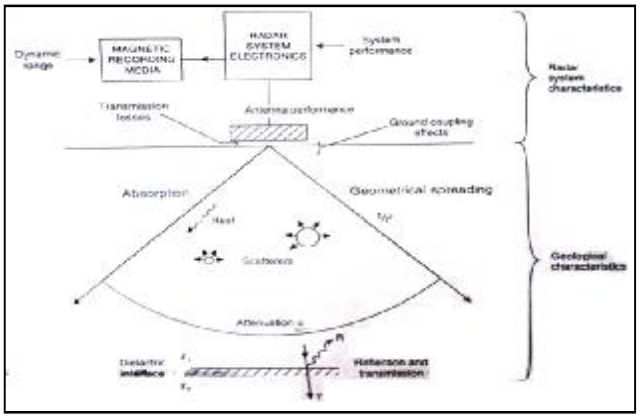

Figure (3) Losses in signal strength [8].

Figure (4) Satellite image for the hole site (Google Earth, 2005).

Figure (5) The early stage of the excavated hole.

(a) First layer at depth 1.25 m

(b) Second layer at depth 0.85 m

(c) Third layer at depth 0.45 m

(d) A schematic diagram for the configuration

Figure (6). Field stages at Turning Unit site with a schematic diagram of the three layers in the hole.

(a) The hole at rainy condition (3-2-2011)

(b) the hole in the sunny condition (13-3-2011)

(c) Investigating the hole site

Figure (7). Field conditions and investigating the site by GPR.

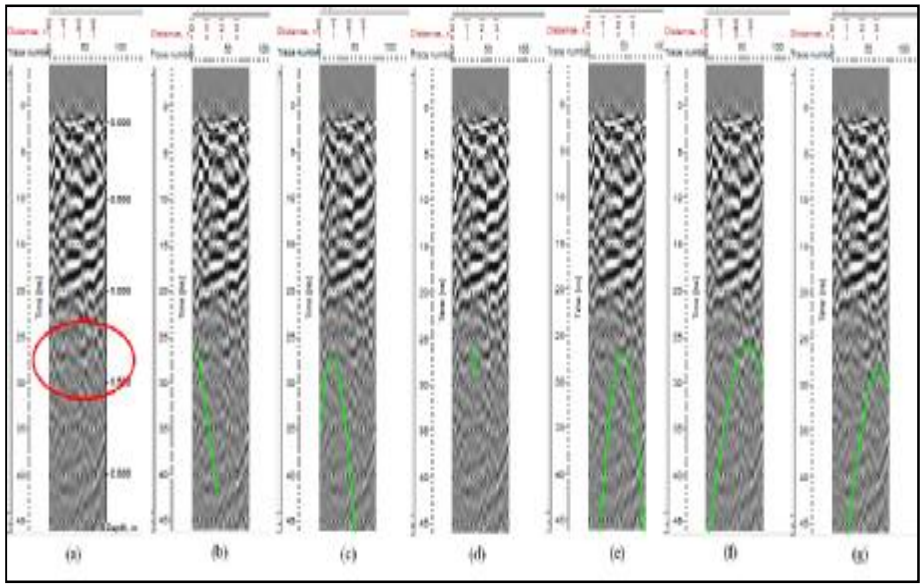

Figure(8). First layer radargrams for buried bodies using 500 MHz processed by Rad Explorer software. (a) The buried bodies (b) Plastic pipe (c) Ferrous pipe (d) Woody prism (e) Reinforced beam (f) Concrete cubes (g) Glass plate.

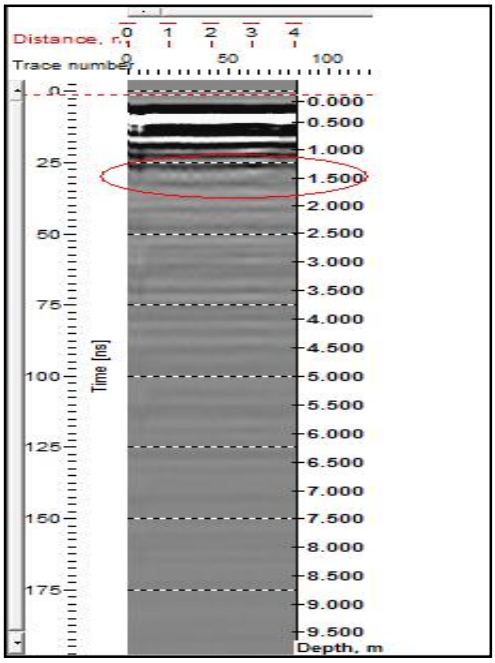

Figure (9) First layer raw data using 250 MHz antenna in the hole site.

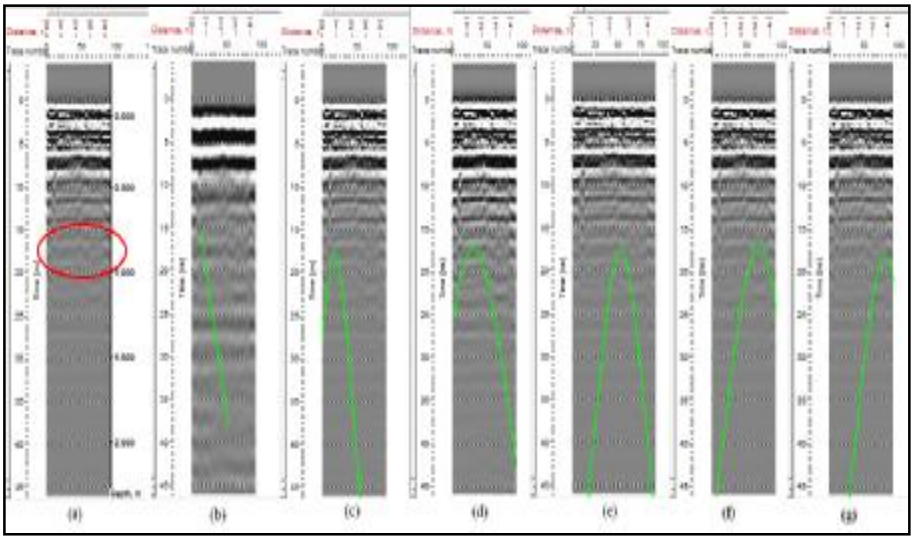

Figure (10). Second layer Radargrams for buried bodies using 500 MHz processed by RadExplorer software. (a) The buried bodies (b) Plastic pipe (c).

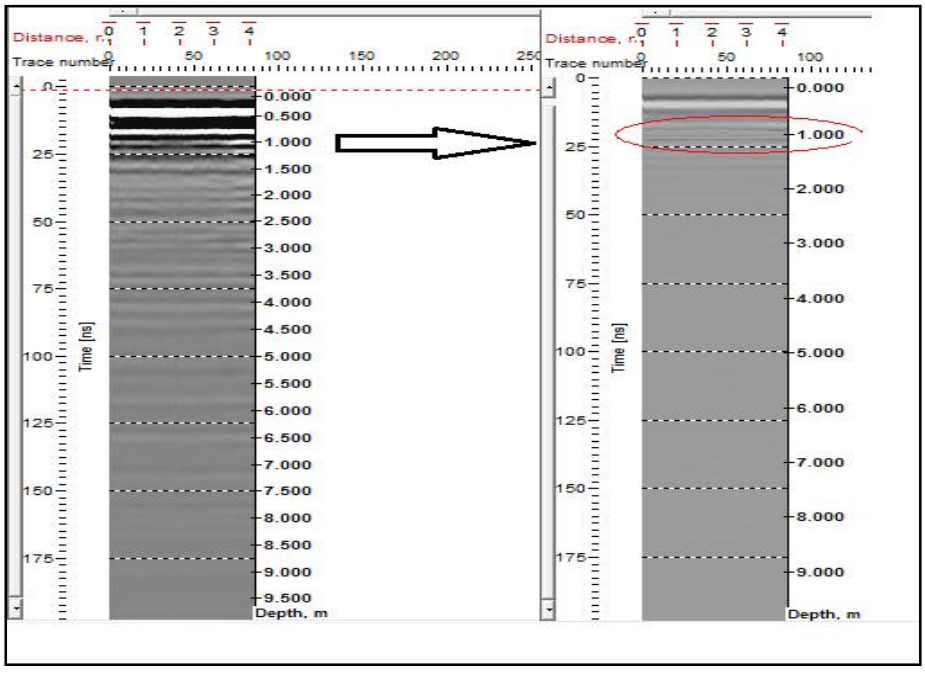

Ferrous pipe (d) Woody prism (e) Reinforced beam (f) Concrete cubes (g) Glass plate.

Figure (11) Second layer radargrams with 250 MHz antenna. Before processing (left side) and after processing (right side).

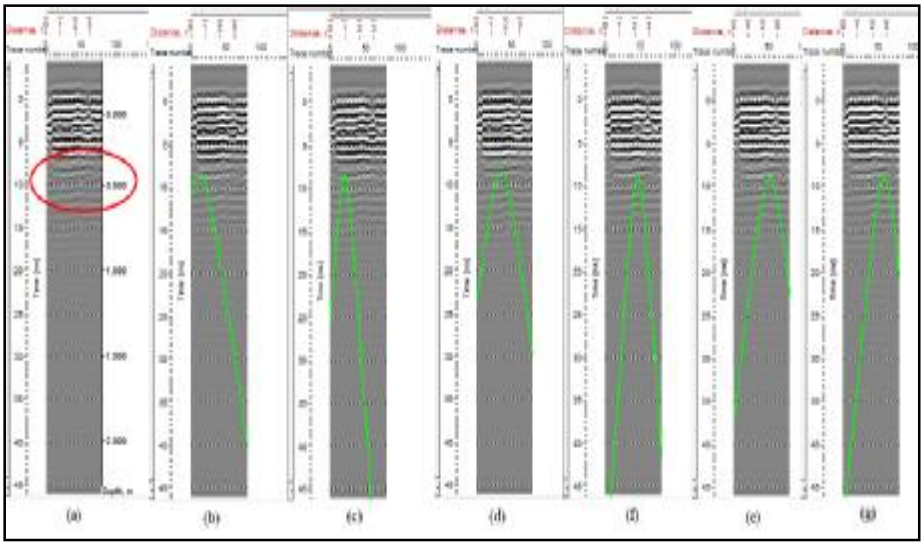

Figure (12) Third layer radargrams fore buried bodies using 500 MHz processed by Rad Explorer software. (a) The buried bodies (b) Plastic pipe.

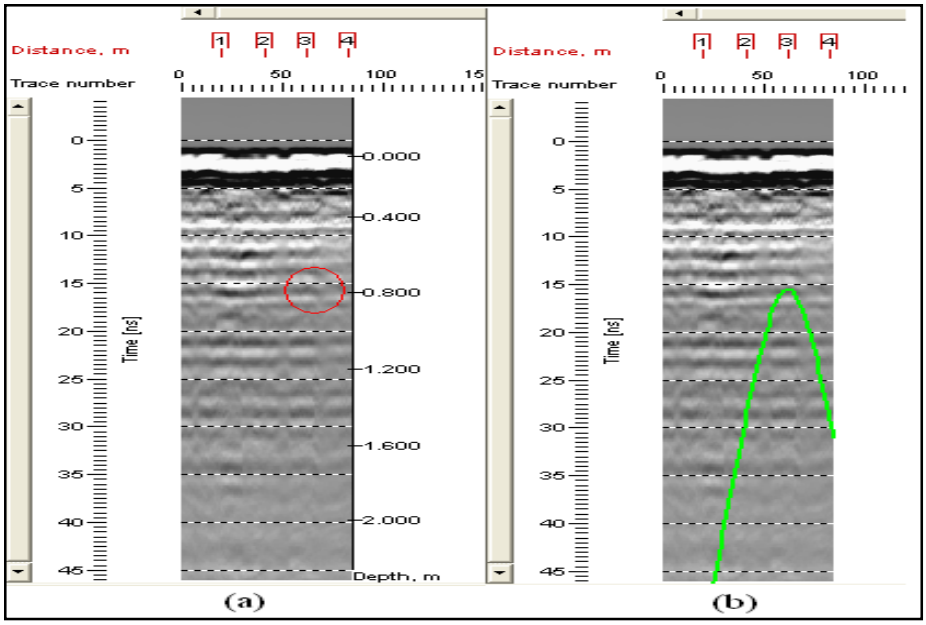

(c) Ferrous pipe (d) Woody prism (e) Reinforced beam (f) Concrete cubes (g) Glass plate.

Figure (13) Third layer radargrams using 250 MHz antenna. Before processing (left side) and after processing (right side).

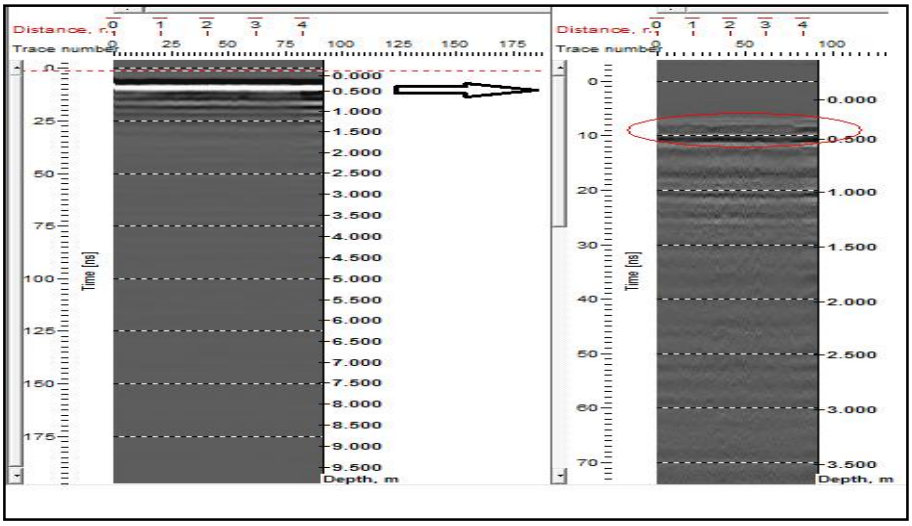

Figure (14) (a) Iron sewage pipe; (b) hyperbola matching for sewage pipe.